Toxicology Letters 388 (2023) 30–39

Contents lists available at ScienceDirect

Toxicology Letters

journal homepage: www.journals.elsevier.com/toxicology-letters

Predicting acute paraquat toxicity using physiologically based kinetic modelling incorporating *in vitro* active renal excretion *via* the OCT2 transporter

Annelies Noorlander *, Sebastiaan Wesseling, Ivonne M.C.M. Rietjens, Bennard van Ravenzwaay

Division of Toxicology, Wageningen University, Stippeneng 4, 6708 WE Wageningen, the Netherlands

ARTICLE INFO

Editor: Angela Mally

Keywords:
Acute toxicity
New approach methodologies (NAM)
Physiologically based kinetic (PBK) modeling
Paraquat
Active renal excretion
Scaling factor
Quantitative *in vitro- in vivo* extrapolation (QIVIVE)

ABSTRACT

Including active renal excretion in physiologically based kinetic (PBK) models can improve their use in quantitative *in vitro- in vivo* extrapolation (QIVIVE) as a new approach methodology (NAM) for predicting the acute toxicity of organic cation transporter 2 (OCT2) substrates like paraquat (PQ). To realise this NAM, kinetic parameters Vmax and Km for *in vitro* OCT2 transport of PQ were obtained from the literature. Appropriate scaling factors were applied to translate the *in vitro* Vmax to an *in vivo* Vmax. *in vitro* cytotoxicity data were defined in the rat RLE-6TN and L2 cell lines and the human A549 cell line. The developed PQ PBK model was used to apply reverse dosimetry for QIVIVE translating the *in vitro* cytotoxicity concentration-response curves to predicted *in vivo* toxicity dose-response curves after which the lower and upper bound benchmark dose (BMD) for 50% lethality ($BMDL_{50}$ and $BMDU_{50}$) were derived by applying BMD analysis. Comparing the predictions to the *in vivo* reported LD_{50} values resulted in a conservative prediction for rat and a comparable prediction for human showing proof of principle on the inclusion of active renal excretion and prediction of PQ acute toxicity for the developed NAM.

1. Introduction

For some compounds the absorption, distribution, metabolism and excretion (ADME) characteristics are substantially influenced by active transport in for example the intestine, kidneys, liver, placenta or the blood-brain-barrier. Incorporating this active transport into physiologically based kinetic (PBK) models based on *in vitro* data is still in a developing stage (Kasteel et al. 2021; Noorlander et al. 2021a; Noorlander et al. 2021b; Noorlander et al. 2022; Poirier et al. 2009; Strikwold et al. 2017; Worley and Fisher, 2015). The challenges related to incorporation of active transport are for example the type of *in vitro* models to be used to quantify the kinetics of the active transporters involved and the scaling factors needed to translate *in vitro* obtained data to the *in vivo* situation. Recent work by our group (Noorlander et al. 2021b) using the herbicide mepiquat (MQ) chloride as the model compound showed that an *in vitro* model using the renal proximal tubule epithelial cell (RPTEC) line SA7K with maintained expression of functionally active transporters (Li et al. 2017) can be useful to quantify PBK model parameters for active transport *via* the organic cation transporter 2 (OCT2). The obtained *in vitro* Michaelis-Menten kinetic parameter values Vmax and Km for this OCT2 mediated transport in the SA7K cells were scaled to the *in vivo* situation and incorporated into a PBK model that was able to adequately predict the time-dependent blood concentrations of MQ only when taking this active OCT2 mediated transport into account (Noorlander et al. 2021b).

A subsequent step would be to extend this first proof of principle and evaluate the use of the SA7K cell model and the defined scaling factor to predict the *in vivo* kinetics of another OCT2 substrate. The first aim of the present study was to provide this further proof of principle using paraquat (PQ) dichloride (N,N′-dimethyl-4,4′-bipyridinium dichloride) (Fig. 1) as the model compound.

PQ is a herbicide belonging to the bipyridylium quaternary ammonium herbicide family. The ADME characteristics of PQ include a rapid but incomplete (5%) absorption from the small intestine followed by its distribution over the tissues and the systemic circulation (Dinis-Oliveira et al. 2008; Houze et al. 1990). PQ is hardly metabolised and systemically eliminated unchanged *via* the kidneys using active transport in addition to glomerular filtration (Chan et al. 1997; Dinis-Oliveira et al. 2008), making it a suitable model substrate for the aim of the present study.

* Corresponding author.
E-mail address: annelies.noorlander@wur.nl (A. Noorlander).

https://doi.org/10.1016/j.toxlet.2023.10.001
Received 23 October 2022; Received in revised form 14 September 2023; Accepted 4 October 2023
Available online 6 October 2023

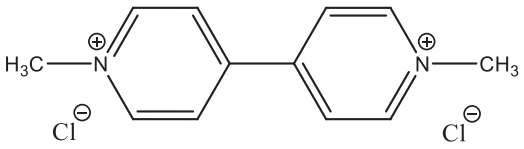

Fig. 1. Molecular structure of paraquat (PQ) dichloride.

Given the cationic nature of PQ the active transporters mainly involved in the renal excretion of PQ are the uptake transporter OCT2 and the multidrug and toxin compound extrusion (MATE) efflux transporter (Chen et al. 2007; George et al. 2017). Several studies reported the activity of OCT2 and MATE for PQ transport, but it remains to be evaluated to what extent OCT2 mediated secretion affects the total plasma clearance *in vivo* (Chan et al. 1998; Chen et al. 2009; Chen et al. 2007). This is also illustrated by the fact that previous PBK models for PQ ignored this active excretion component deliberately assuming that glomerular filtration of PQ would suffice for the model predictions (Campbell et al. 2021; Lohitnavy et al. 2017; Stevens et al. 2021).

The use of PQ as a weed killer has been banned in many countries due to its toxic properties where exposure mainly originates from accidental or intentional ingestion, or exposure *via* damaged skin (occupational) or inhalation (Watts, 2011) and may lead to death. The US Environmental Protection Agency (EPA) reported in 2019 on an oral no observed adverse effect level (NOAEL) of 0.5 mg paraquat ion/kg bw/day based on the incidence of gross lung lesions, increased lung weight and severity of chronic pneumonitis in two co-critical subchronic and chronic dog oral toxicity studies (EPA U, 2019). With the uncertainty factors for inter- and intraspecies variability this NOAEL resulted in a health based guidance value (HBGV) of 0.005 mg paraquat ion/kg bw/day. Acute toxicity in rat and human has been reported to result from accumulation and toxicity of PQ in lung tissue and to occur at mean lethal dose levels (LD_{50}) ranging between 40 and 200 mg/kg bw and 3 – 60 mg/kg bw, respectively (Dinis-Oliveira et al. 2008; Roberts JRRR, 2013; Watts, 2011).

In the past many (fatal) cases have been reported associated with accidental and particular intentional ingestion of PQ. The case studies reported provide limited information on exposure and time of admission to the hospital after ingestion. One study reported on the ingested PQ dose in grams and several other studies report the dose in terms of the percentage of PQ in the ingested formula (Houze et al. 1990; Proudfoot et al. 1979; Sawada et al. 1988). Once admitted in the hospital blood samples were taken and measured regularly until patients died or in some cases survived. Proudfoot et al. (1979) collected these data of 71 cases and generated a time-dependent blood concentration survival curve for the first 24 h following ingestion where all cases with blood levels reported below this curve would survive the exposure to PQ. This survival curve has been extended to days after ingestion by Scherrmann et al. (1987) using a hyperbolic equation. Defining a dose-response curve for PQ acute toxicity in human using a PBK model based New Approach Methodology (NAM) would support the evaluation of the hazards and risks of PQ exposure based on external as well as internal dose levels.

Thus, the aim of the present study was to predict the acute toxicity of PQ *via* quantitative *in vitro- in vivo* extrapolation (QIVIVE) as a NAM. Hereto, a PBK model that includes *in vitro* kinetic data for active renal excretion of PQ *via* the OCT2 transporter will be developed and used to translate *in vitro* cytotoxicity concentration-response data obtained from rat lung epithelial cell lines (RLE-6TN and L2)) and a human lung epithelial cell line (A549) into *in vivo* dose-response data *via* PBK modelling based reverse dosimetry. The predicted dose response curves will be compared to available toxicity data to further evaluate the PBK model and predictions made. The results will at the same time provide insight into the role of active renal excretion in the kinetics of PQ and enable definition of a point of departure for evaluation of the acute toxicity of PQ.

2. Materials and methods

2.1. Chemicals

Paraquat (PQ) dichloride hydrate, ammonium formate, bovine serum albumin (BSA) and formic acid were purchased from Sigma-Aldrich (Zwijndrecht, the Netherlands). Hydrochloride acid (HCl) was purchased from Merck (Darmstadt, Germany). Doxepin hydrochloride was purchased from Carbosynth (Berkshire, UK). Dimethyl sulfoxide (DMSO) used for dissolving doxepin was purchased from Merck (Darmstadt, Germany). Acetonitrile and methanol were purchased from Biosolve (Valkenswaard, the Netherlands). Ultrapure water was used from a system of Arium Pro VF Sartonius (Rotterdam, the Netherlands).

2.2. Cell culture

2.2.1. Lung cell line

The (immortalized) rat lung epithelial cell line (RLE-6TN) (ATCC® CRL-2300™, Wesel, Germany) was cultured in Ham's F12 medium supplemented with 10 μg/mL bovine pituitary extract, 2 mM L-glutamine, 1% penicillin/streptomycin, 30 μg/mL gentamicin (all from Thermo Fischer Scientific Bleiswijk, the Netherlands), 5 μg/mL insulin (Sigma-Aldrich, Zwijndrecht, the Netherlands), 1.25 μg/mL transferrin, 10% foetal bovine serum (FBS) (both from Capricorn, Leusden, the Netherlands), 2.5 ng/mL recombinant rat insulin-like growth factor (BioTechnology, Abingdon, U.K.), 2.5 ng/mL epidermal growth factor (Lonza, Breda, the Netherlands) at 37 °C with 5% (v/v) CO_2 and 95% (v/v) humidity. Cells used in this study were between 2 and 11 cell passages. In this study all concentrations and doses of PQ relate to its dichloride salt form.

2.2.2. Kidney cell line

The human renal proximal tubule epithelial cell (RPTEC) line SA7K (Sigma-Aldrich, Zwijndrecht, the Netherlands) was cultured in MEMα (Sigma-Aldrich, Zwijndrecht, the Netherlands) supplemented with RPTEC Complete Supplement (Sigma-Aldrich, Zwijndrecht, the Netherlands), 2.5 mM L-glutamine, 30 μg/mL gentamicin and 0.015 μg/mL amphotericin B (all from Thermo Fischer Scientific Bleiswijk, the Netherlands) at 37 °C with 5% (v/v) CO_2 and 95% (v/v) humidity. For uptake studies cells were seeded in 6-well plates at a density of 5×10^5 – 7.5×10^5 cells/well and grown for 2 days prior to use with a medium change after one day. Cells used in this study were between 7 and 17 cell passages.

2.3. Cytotoxicity of PQ

2.3.1. Experimental

RLE-6TN cells were seeded in 96-well plates at a density of 1×10^4 cells/well and after a 24 h incubation for cell attachment the cells were exposed to PQ (final concentrations 5, 10, 25, 50, 75, 100, 125, 150, 175 and 200 μM) (added from 200 times concentrated stock solutions in ultrapure water) for 24 h. Then 5 μL water soluble tetrazolium-1 (WST-1) was added to each well and the cells were incubated for an hour at 37 °C. Finally, the absorbance was measured at two wavelengths (440 nm; 620 nm) using a microplate reader (SpectraMax® iD3). Each concentration was tested in sextuplet with a biological replicate of four times. The data were calculated as percentage of the solvent control.

2.3.2. Literature

Additional *in vitro* cytotoxicity data of PQ were collected from the literature. Three more studies reported on the PQ cytotoxicity in RLE-6TN cells (Wang et al. 2016; Wang et al. 2018; Zhu et al. 2016). One study reported on PQ cytotoxicity in another immortalized rat lung cell line L2 (Chen et al. 2012). All reported studies exposed the cells for 24 h. Furthermore, PQ cytotoxicity data collected in the human adenocarcinoma cell line A549 were reported in four studies where three studies

exposed the cells for 24 h and two studies for 48 h (Kanno et al. 2019; Kim et al. 2011; Wang et al. 2016; Zhu et al. 2016).

2.4. OCT2 uptake of PQ

2.4.1. Experimental

SA7K cells were pre-incubated in pre-warmed (37 °C) uptake buffer (136 mM NaCl, 5.3 mM KCl, 1.1 mM KH_2PO_4, 0.8 mM $MgSO_4{\cdot}7\ H_2O$, 1.8 mM $CaCl_2{\cdot}2\ H_2O$, 11 mM D-glucose, 10 mM HEPES, pH 7.4) within the presence or absence of the OCT2 inhibitor doxepin (Chan et al. 1998; Hacker et al. 2015; Li et al. 2017; Samai et al. 2008) (final concentration 100 μM added from a 200 times concentrated stock solution in DMSO) for 10 min at 37 °C. After 10 min, PQ (final concentration 10 μM added from a 200 times concentrated stock solution in methanol:HCl 0.1 M (1:1)) was added and the cells were incubated for 2, 5, 10, 15, 30 and 60 min. Each experimental condition was measured in a technical triplicate and a biological duplicate. After incubation, medium was removed and cells were washed twice with ice-cold PBS containing 0.2% (w/v) BSA and once with ice-cold PBS alone (to eliminate unspecific binding). Cells were lysed with methanol:HCl 0.1 M (1:1) in a freeze-thaw cycle. Protein was measured using the Pierce BCA protein assay kit (Thermo Fischer Scientific Bleiswijk, the Netherlands). PQ present in the cell lysate was quantified using LC-MS/MS. It is also important and crucial to note that at all times polypropylene/polystyrene materials were used for PQ, because of its ability to adsorb to glass (Muhamad et al. 2011).

2.4.2. Literature

A literature search was done in PubMed to collect all the available *in vitro* kinetic data on OCT2 transport of PQ reporting the Km and Vmax using search strings: (Paraquat[Title/Abstract]) AND (organic cation [Title/Abstract]), Paraquat[Title/Abstract]) AND (OCT2[Title/Abstract]), (paraquat) AND (Vmax) AND (organic cation), (Paraquat[Title/Abstract]) AND (hOCT2), (Paraquat[Title/Abstract]) AND (Vmax[Title/Abstract]) AND (Transport[Title/Abstract]) (search date: 13.1.2023). Upon evaluation of the search outcomes there was but one study remaining that contained the necessary information. That study provided two reported data sets (Vmax and Km) on the OCT2 specific transport of PQ in human embryonic kidney (HEK) 293 cells overexpressing the OCT2 transporters in one study (Chen et al. 2007).

2.5. Liquid chromatography mass spectrometry (LC-MS/MS)

For quantification of PQ the protocol described by Pizzutti et al. (2016) was used. In brief, PQ was quantified on an LC-MS/MS system (Shimadzu, Kyoto, Japan), containing a Nexera XR LC-20AD SR UPLC system coupled to a triple quadrupole mass spectrometer LCMS-8040 with a Sielc Obelisc R column (100 ×2.1 mm, 5 μm particle size). The mobile phase consisted of (A) 20 mM ammonium formate with formic acid (pH 3.0) and (B) acetonitrile with 0.1% (v/v) formic acid (gradient: 0.00–5.50 min 80–20% B, 5.50–8.50 min 20% B, 8.50–11.50 min 20–80% B, 11.50–14.00 min 80% B). The flow rate was 0.4 mL/min. The injection volume was 5 μL and the column oven was set at 40 °C. Under these conditions the retention time of PQ was 7.0 min. The mass spectrometer was set in the positive electron spray mode. The MRM transitions used to determine and quantify PQ were 186.2 → 171.0, 186.2 → 77.0 and 186.2 → 155.0 (*m/z* for all masses).

2.6. Physiologically based kinetic (PBK) modelling

A physiologically based kinetic model for PQ was developed for rat and human. The models consisted of separate compartments for GI-tract, kidney, lung, liver, fat and blood (Fig. 2). The rest of the organs/tissues were placed either under rapidly perfused tissue (brain, heart) or slowly perfused tissue (bone, skin, muscle). The parameters for tissue weight and tissue blood flow were collected from Brown et al. (1997). The QIVIVE toolbox developed by Punt et al. (2020) was used to obtain

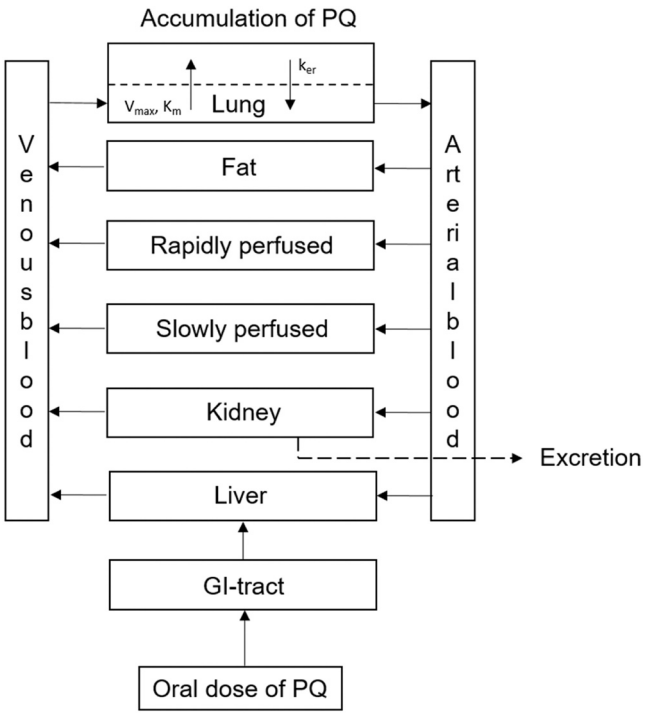

Fig. 2. Schematic overview of the conceptual PBK model for PQ including renal excretion and active uptake in lung tissue.

tissue:blood partition coefficients based on Rodgers and Rowland (2006). Toolbox input of PQ: LogP = −4.22, molecular weight = 257.2 g/mol, ticked box for the presence of quaternary N atom(s) (Supplementary Table A.1 for overview of parameters). Only 5% of the orally administered PQ crosses the GI-tract into the blood in rat, which in the case of humans is around 10% (Houze et al. 1990). Absorption rate was fitted to the data for rat (ka = 2.3 hr^{-1}) and kept the same for human due to absence of data. Transport of PQ into the alveolar tissue *via* the polyamine uptake system is incorporated in the model *via* the Michaelis-Menten parameter values Vmax (300 nmol/g tissue/h for both rat and human) and Km (70 and 40 μM for rat and human, respectively) derived from a study with lung slices (Dinis-Oliveira et al. 2008). The accumulation is simulated based on these active uptake parameters with inclusion of a low transport rate back into the lung blood (k_{er}= 0.003 hr^{-1}) (Lohitnavy et al. 2017). PQ is hardly metabolised in the body (Lock, 2010), therefore no equations and kinetic parameters for hepatic clearance were included in the model. In the PBK model the clearance of PQ is completely depending on glomerular filtration and active transport *via* OCT2 in the kidney, which in the model is described as follows:

$$AKe = (GFR \times (CVK \bullet Fub)) + \left(\frac{Vmax_{OCT2} \times (CVK * Fub)}{(Km_{OCT2} + (CVK * Fub))}\right) \quad (1)$$

where AKe is the amount of PQ excreted *via* the kidney over time (μmol/hr), GFR is the glomerular filtration rate (L/hr), (rat; 0.078 L/hr, human; 7.56 L/hr (Walton et al. 2004)) CVK the venous concentration of PQ in the kidney (μmol/L), $Vmax_{OCT2}$ and Km_{OCT2} the maximum rate (μmol/hr) and Michaelis-Menten constant (μmol/L) for the active transport of PQ by OCT2, and Fub the fraction unbound of PQ in blood, which was 0.7 for rat and 0.65 for human (Stevens et al. 2021). Berkeley Madonna software (UC, Berkeley, CA, USA version 10.2.8) was used to solve the equations with the Rosenbrock-stiff model.

2.7. Scaling factor

Conversion of the *in vitro* obtained Vmax value for OCT2 uptake of

PQ in SA7K cells expressed in pmol/min/mg protein into an *in vivo* Vmax expressed in μmol/hr/kidneys is done with a scaling factor, which has been extensively elaborated on in our previous work (Noorlander et al. 2021b). Briefly, the scaling factor consisted of three parts. 1) Converting the activity in the cells *in vitro* expressed in pmol/min/mg cellular protein to the activity expressed in a unit that represents the activity in the two whole kidneys expressed in pmol/min/g kidneys. 2) Including only the part of the kidney – kidney cortex - where OCT2 is expressed. 3) Scaling to account for the fact that the expression and activity of OCT2 in the *in vitro* system differs from its expression and activity in the renal tubule cells in the kidney cortex, which includes: i) the differences in OCT2 expression levels, ii) potential differences in membrane potential between the relevant cells *in vitro* and *in vivo* and, iii) interspecies differences between human (SA7K/HEK293 cell line) and rat (the PBK model). Fitting the *in vitro* obtained Vmax in Berkeley Madonna to available *in vivo* data informed on the actual size of this third part of the scaling factor. The overall scaling factor was acquired by multiplying the three factors. For conversion of the *in vitro* Vmax for OCT2 mediated transport of PQ to the *in vivo* Vmax for OCT2 mediated transport the following formula was used:

$$In\ \ vivo\mathrm{Vmax} = \left(\frac{In\ \ vitro\mathrm{Vmax}}{1,000,000}\right) \times 60 \times \mathrm{SF} \times (\mathrm{Volume\ of\ kidneys}) \times 1000 \tag{2}$$

where the factor 1000,000 is used to convert pmol to μmol, 60 to convert minutes to hours, 1000 to convert kg kidney weight to g kidney weight and SF is the scaling factor encompassing the three parts mentioned above expressed in mg protein/g kidney.

The full model code is presented in the Supplementary materials.

2.8. Evaluation of the PBK model and sensitivity analysis

The developed PBK model for PQ in rat was evaluated by comparing the predicted oral blood concentration time curve with available experimental data on the blood concentration time curve of PQ in rat at non-toxic levels (0.039 mg/kg bw) (Chui et al. 1988). The root mean square error was used to compare different model outcomes with the available experimental data. To quantify the contribution of active renal excretion *via* OCT2 to the overall clearance of PQ, the PBK model-predicted blood concentration time curve was compared with the predicted blood concentration time curve obtained with only passive glomerular filtration. For human, the focus was on the blood concentration time curves of the patients who survived the PQ exposure (Proudfoot et al. 1979). However, most of the literature studies reporting blood-concentration time curves did not quantify the starting dose. Only Houze et al. (1990) reported on the dose of survivors which was between 0.5 and 0.8 g. Translating these doses back to doses in mg/kg bw taking 70 kg as the average bodyweight, survivors took 7.1–11.4 mg/kg bw. Blood concentration time curves were predicted at these doses assuming the model was well validated for rat and therefore suitable for human (Supplementary data Fig A.1).

To identify the model parameters with the highest influence on the model output (maximum blood concentration (C_{max})) a sensitivity analysis was performed. The sensitivity analysis was performed at the dose level used in the available rat study (0.039 mg/kg bw). Normalised sensitivity coefficients (SCs) were calculated for the model parameters based on the method reported in the literature (Evans and Andersen, 2000) as follows:

$$SC = \frac{C' - C}{P' - P} \times \left(\frac{P}{C}\right) \tag{3}$$

were C is the initial value of the model output, C′ is the modified value of the model output resulting from an increase in the parameter value. P is the initial parameter value and P′ is the modified parameter value after a 5% increase in its value. (Supplementary data Fig A.2).

2.9. Translation of the in vitro cytotoxicity data of PQ to in vivo dose response data

2.9.1. Determining fraction unbound in vitro

The obtained concentration-response data for the cytotoxicity of PQ in RLE-6TN, L2 and A549 cells were used to predict the dose levels that are required to reach the respective effect concentrations of PQ in blood, using PBK modelling-based reverse dosimetry. Important to realize is that only the free fraction of the compound will exert the effects, meaning that a correction is required for differences in protein binding in the *in vitro* and *in vivo* situation prior to applying reverse dosimetry. Therefore, the fraction unbound *in vitro* ($f_{ub\ in\ vitro}$) and the fraction unbound *in vivo* ($f_{ub\ in\ vivo}$) needed to be determined. Although it has been reported frequently that the $f_{ub\ in\ vivo}$ of PQ is 1.0 due to its two quaternary positively charged N-atoms, a thoroughly executed protein binding assay recently performed by the group of Campbell (Campbell et al. 2021; Stevens et al. 2021) reported the $f_{ub\ in\ vivo}$ of PQ to be 0.7 and 0.65 for rat and human, respectively. To determine the $f_{ub\ in\ vitro}$ a previously reported method by van Tongeren et al. (2021) was used where a linear relation between the fraction unbound and the protein content in a biological matrix was assumed based on the work of Gulden et al. (2002). This means that the fraction unbound in the absence of protein is 1.0. The protein content is reported to be 7% in rat plasma and 8% in human plasma (Martinez, 2011; Mathew et al. 2022). However, the PBK model is run for whole blood, therefore the percentages need to be recalculated. Blood plasma is around 60% of whole blood (Dean, 2005) so a dilution factor of 100/60 = 1.67 is used to calculate a whole blood protein content of 4.2% for rat and 4.8% for human. The assay medium used in all the cytotoxicity assays contained 10% FCS and was considered to be a 10% protein content. Based on these considerations, the $f_{ub\ in\ vitro}$ for PQ was calculated by linear extrapolation to the 10% protein content using the f_{ub} of 1.0 in the absence of protein and the respective $f_{ub\ in\ vivo}$ value from Campbell et al. (2021) and Stevens et al. (2021) of 0.7 and 0.65 for a 4.2% protein content in rat *in vivo* blood and an 4.8% protein content in human *in vivo* blood, respectively, and found to amount to 0.29 for rat and 0.27 for human.

2.9.2. PBK modelling-based reverse dosimetry

Pneumotoxicity was assumed to depend on the maximum unbound concentration (C_{max}) of PQ reached in the blood and is therefore the chosen dose metric in this study for reverse dosimetry (Rietjens et al. 2019). This means that the predicted C_{max} is plotted against the dose from which a formula $y = ax$ can be derived (Supplementary data Fig A.3.). For reverse dosimetry, first the predicted C_{max} was corrected for the difference in protein binding in the *in vitro* and *in vivo* situation. To this end the *in vitro* unbound concentration ($C_{ub,\ in\ vitro}$) which equals $C_{in\ vitro} \times f_{ub,\ in\ vitro}$ was set equal to the unbound C_{max} in blood ($C_{ub,\ in\ vivo}$) which equals the predicted $C_{max} \times f_{ub,\ in\ vivo}$, so that the following equations holds: Predicted $C_{max} = C_{in\ vitro} \times (f_{ub,\ in\ vitro} / f_{ub,\ in\ vivo})$. Using this formula the $C_{in\ vitro}$ was converted to a corresponding predicted C_{max} which, using the plots of the predicted C_{max} *versus* the dose (Supplementary data Fig A.3.) can be converted to a dose. Then at these calculated dose levels the effect was assumed to be similar to the effect at the corresponding concentration in the *in vitro* concentration response curve.

The same steps were applied to *in vitro* concentration-response curves obtained for PQ in RLE-6TN cells, L2 cells and the human A549 cells in previously reported studies (Chen et al. 2012; Kanno et al. 2019; Kim et al. 2011; Wang et al. 2016; Zhu et al. 2016). The contribution of including active renal secretion *via* OCT2 to the PBK model was evaluated by translating the *in vitro* concentration-response curves with the PBK model with or without taking active transport in the kidney into account.

2.10. Point of departure for acute toxicity of PQ

For the obtained and literature found *in vitro* concentration response curves in the different cell lines EC_{50} and ED_{50} values were derived by interpolating the exponential or sigmoidal function. In this case 50% viability is considered to be reached at the EC_{50}/ED_{50}. Upon translation using PBK model based reverse dosimetry Benchmark dose (BMD) analysis was applied on the predicted *in vivo* dose response curves using the European Food Safety Authority (EFSA) online BMD software. The lower and upper bound BMD levels for 50% lethality ($BMDL_{50}$ and $BMDU_{50}$) were determined under the EFSA default settings for Akaike information criterion being 2 and a confidence interval of 95%. Only $BMDL_{50}$ and $BMDU_{50}$ values as a result of model averaging were taken. The obtained $BMDL_{50}$-$BMDU_{50}$ ranges were compared to respectively the *in vivo* reported LD_{50} values collected from the literature for both rat and human.

3. Results

3.1. Cytotoxicity of PQ

Exposure of the RLE-6TN cells to PQ resulted in a concentration dependent decrease in cell viability (Fig. 3a; black data) with an EC_{50} established at 128 μM. Comparing the results to existing literature data reveals that these results are well in line with reported EC_{50} values that range from 79 to 166 μM, (Fig. 3a; red data and blue data, respectively). The literature data reported by Wang et al. (2018) were not considered and not included in Fig. 3a as the cell viability did not reach and extend past the 50% cell viability. In comparison, cytotoxicity data of another rat lung cell line, the L2 cell line, (Fig. 3b) shows this latter cell line to be less sensitive to PQ with an EC_{50} of 319 μM.

The literature reported *in vitro* data for the human lung cell line A594 resulted in an EC_{50} range of 400 to 889 μM when exposed to PQ for 24 h (Kim et al. 2011; Wang et al. 2016; Zhu et al. 2016) (Fig. 4a) and a 4- to 12-fold lower EC_{50} range of 72 to 97 μM upon 48 h PQ exposure (Kanno et al. 2019; Kim et al. 2011) (Fig. 4b).

3.2. Uptake of PQ in the SA7K cells

Fig. 5 presents the time dependent uptake of PQ in SA7K cells in the absence and in the presence of the OCT2 inhibitor doxepin. These data reveal that PQ is taken up by the SA7K cells (black solid line) with this uptake being inhibited in the presence of doxepin (grey solid line). The difference between the curves in the absence or presence of the inhibitor reveals that the OCT2 mediated uptake of PQ (black striped line) amounts on average to 42% of the total uptake. The data also reveal that uptake does not increase in time hampering quantification of the rate of uptake (in pmol/min/mg protein) from a linear part of the concentration-time curve.

3.3. Kinetic data from literature

As the rate of PQ uptake in the SA7K cell line appeared too fast to determine the PQ concentration dependent rate of transport, Vmax and Km for PQ uptake *via* OCT2 were obtained from literature. Two data sets were reported by Chen et al. (2007) using the HEK293 cell line over-expressing the human OCT2 transporter (Km: 95 μM and 114 μM and Vmax: 198 pmol/min/mg protein and 174 pmol/min/mg protein). To further optimize the PBK model predictions with incorporation of *in vitro* OCT2 uptake of PQ the data of the HEK293 cells were used and averaged (Km: 104.5 μM and Vmax: 186 pmol/min/mg protein).

3.4. Evaluation of the model and defining the scaling factor

The PBK model was evaluated based on comparison of predicted C_{max} levels for PQ in rats to C_{max} values from *in vivo* kinetic rat data reported by Chui et al. (1988) at an oral dose of 0.039 mg/kg bw (Fig. 6) using different subsequent steps. The first step is based on comparison of the experimental data to the PBK model based predictions including only passive excretion *via* glomerular filtration (GF) in the PBK model (dotted line). The predicted time-dependent concentration curve predicts a C_{max} value for PQ that is 1.5 fold higher than the C_{max} derived from the reported *in vivo* data (open circles) indicating excretion is somewhat underestimated. In a second step active excretion was added to the PBK model using the *in vitro* OCT2 data for PQ transport obtained in HEK293 cells (solid line). The *in vitro* Vmax value (186 pmol/min/mg protein) was scaled to the *in vivo* situation using a scaling factor taking into account the three parts mentioned in the materials and methods Section 2.7. With part one being the reported mg protein/g kidney (300 mg protein/g kidney (Kumar et al. 2018)) and part two the location of OCT2, which is the kidney cortex making up 70% of the kidney weight (300×70%= 210 mg protein/g kidney). Use of this scaling factor is further referred to as partially scaled. The predicted Cmax under these conditions is 1.3 fold higher than the reported *in vivo* data. Given the fact that the scaling factor used did not yet account for differences in expression level of OCT2 in the HEK293 cells and the *in vivo* tubular cells

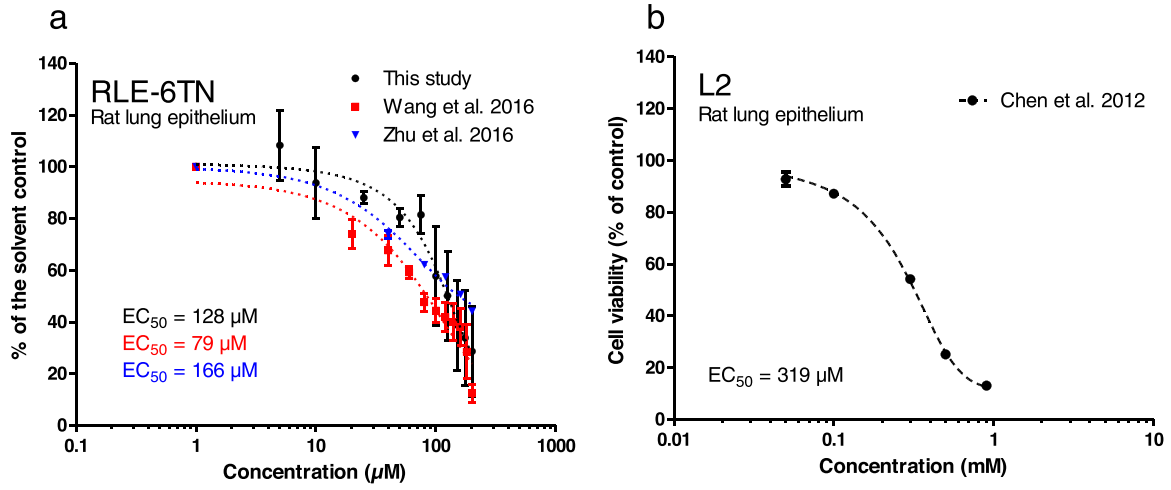

Fig. 3. Cell viability of two rat lung epithelial cell lines after exposure to increasing concentrations of PQ for 24 h expressed as percentage of the solvent control for (a) RLE-6TN cells as determined in this study (EC_{50} 128 μM; black). For comparison the figure also presents previously reported cytotoxicity data reported by Wang et al. (2016) (EC_{50}: 79 μM; red) and Zhu et al. (2016) (EC_{50}: 166 μM; blue) and (b) L2 cells as reported by Chen et al. (2012) (EC_{50}: 319 μM). Data points represent the mean ± SD; n = 3–4 for all data sets.

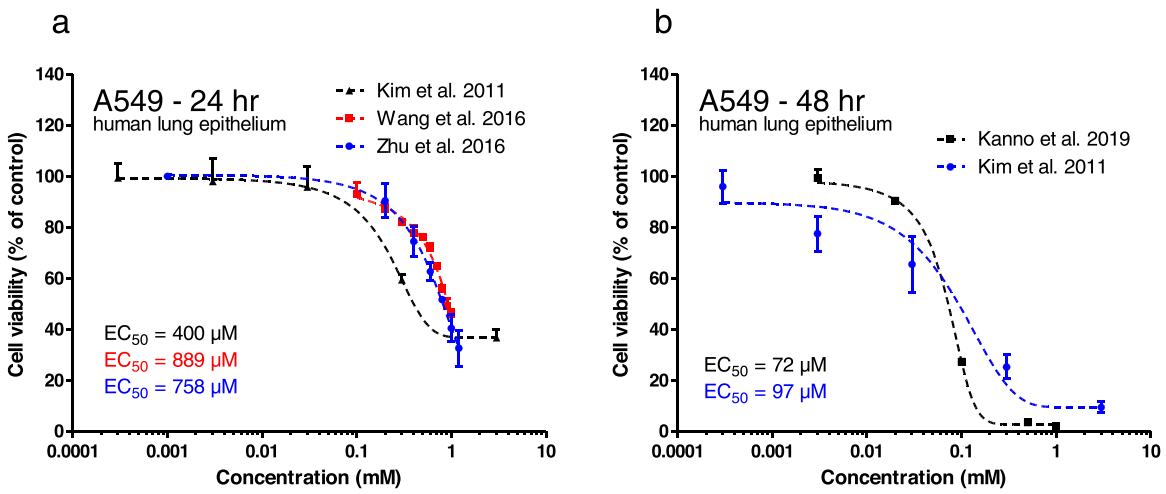

Fig. 4. Cell viability of the human A594 cells expressed as percentages of the solvent control after exposure to increasing concentrations of PQ for (a) 24 h as reported by Kim et al. (2011) (EC_{50}: 400 µM; black), Wang et al. (2016) (EC_{50}: 889 µM; red) and Zhu et al. (2016) (EC_{50}: 758 µM; blue) and (b) 48 h as reported by Kanno et al. (2019) (EC_{50}: 72 µM; black) and Kim et al. (2011) (EC_{50}: 97 µM; blue). Data points represent the mean ± SD; n = 3–6 for all data sets.

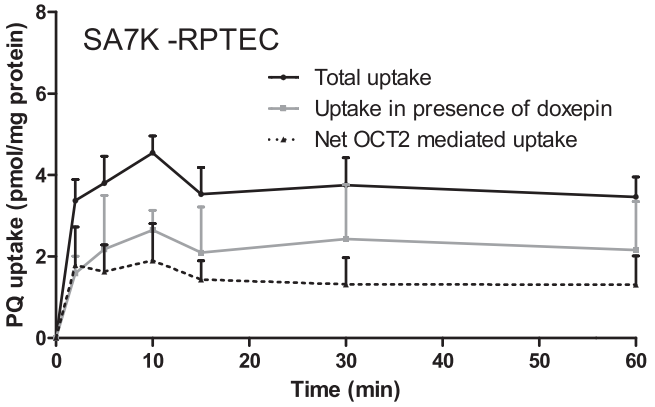

Fig. 5. Time dependent uptake of PQ (10 µM) in SA7K cells in the presence of 100 µM doxepin. The uptake remaining in the presence of the inhibitor (grey solid line) was subtracted from the total uptake (black solid line) to obtain the net OCT2 mediated uptake of PQ (black striped line). Each data point represents the mean ± SEM; n = 2.

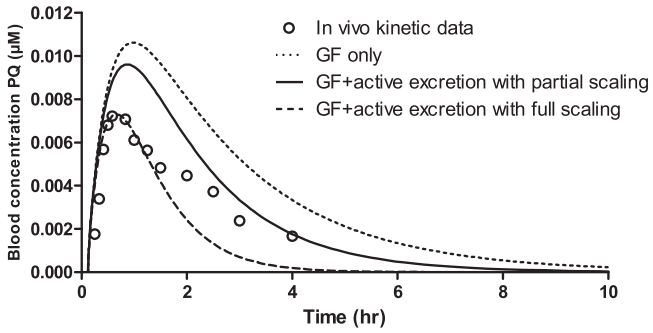

Fig. 6. Predicted blood concentration time curves in rats upon orally administered PQ at dosage 0.039 mg/kg with a bioavailability of 5% as reported by Chui et al. (1988) (open circles). The predictions were executed under the following conditions: 1) with glomerular filtration (GF only) (dotted line), 2) with GF and active excretion, the latter with partial scaling of the *in vitro* OCT2 transport data of PQ in HEK293 cells overexpressing OCT2 reported by Chen et al. (2007) based on the amount of protein/g kidney and fraction of kidney where OCT2 is located (300 mg/g kidney x 0.7) (solid line) and 3) with GF and active excretion, the latter with full scaling also correcting for a 5.5 fold difference in OCT2 expression in the HEK293 cells and kidney cells, resulting in a full scaling factor of 300 mg/g kidney x 0.7 × 5.5 = 1155 mg protein/g kidney used when translating the *in vitro* Vmax to an *in vivo* Vmax.

in a third step the optimised scaling factor was defined fitting the predictions by adjusting the scaling factor parameter to the *in vivo* data. This resulted in an extra scaling factor of 5.5 on top of the 210 mg protein/g kidney and an overall scaling factor of 1155 mg protein/g kidney (210 mg protein/g kidney x 5.5). Eq. (2) would now be Eq. (4):

$$In\ \ vivo\mathrm{Vmax} = \left(\frac{In\ \ vitro\mathrm{Vmax}}{1,000,000}\right) \times 60 \times (300 * 0.7 * 5.5) \times (\mathrm{Volume\ of\ kidneys}) \times 1000 \quad (4)$$

Use of this scaling factor is further referred to it as fully scaled. As reported by our previous work (Noorlander et al. 2021b), here too, the virtual amount of protein exceeds the kidney weight due to the lower expression level of OCT2 in the HEK293 cells as compared to kidney tissue and requires a virtually large amount of HEK293 protein to equal the amount OCT2/g kidney. The predicted time-dependent blood concentration curve of PQ with the fully scaled scaling factor (striped line) adequately describes the reported *in vivo* kinetic data especially within the first phase. The decreased root mean square error calculated indicates the improvement of the model predictions as well (Supplementary Table A.2.) A comparison of the amount of PQ excreted in time reflected by the slope of the glomerular filtration *versus* time curve (0.25 nmol/hr) and the slope of PQ excreted in time by only the scaled active transport (0.7 nmol/hr) showed that the contribution of excretion *via* active transport in time was 1.8 fold higher than that *via* GF. This results in 73% of the urinary PQ being excreted by active excretion at a dose of 0.039 mg/kg bw (Fig. 7). The PBK model also reveals that the relative contribution of OCT2 decreases when the PQ dose increases (at 39 and 390 mg/kg bw active excretion is 67% and 34%, respectively) pointing at saturation of the OCT2 transport. A final comparison was made between the partial scaling and full scaling indicating that the OCT2 contribution in partial scaling was at most 33.5% and also decreased with increasing doses.

Based on the evaluation of the rat model it was assumed that the human PBK model that was developed by the same method and principles would also be adequate. This assumption was supported by the observation that the predicted concentrations for the time dependent blood concentration in human at a non-toxic dose (0.036 mg/kg bw) were all well below Proudfoot's survival curve (see appendix A Fig A.1).

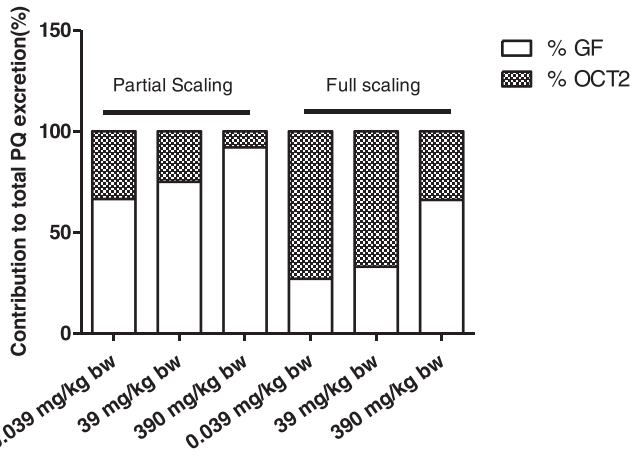

Fig. 7. Contribution (%) of glomerular filtration (GF) and OCT2 mediated excretion to the total amount of PQ excreted as predicted by the PBK model when using different scaling factors. Included are partial scaling of the Vmax (SF; 300 * 0.7 = 210 mg protein/g kidney) and full scaling of the Vmax (SF; 300 ×0.7 ×5.5 = 1.155 mg protein/g kidney). The contributions were predicted at dose levels of 0.039 mg/kg bw, 39 mg/kg bw and 390 mg/kg bw.

3.5. Applying reverse based dosimetry

Using the developed PBK models for rat and human reverse based dosimetry was applied to translate the *in vitro* concentration-response data into *in vivo* dose-response curves (Fig. 8). For rat, the three *in vitro* RLE-6TN data sets and the *in vitro* L2 data set were converted to *in vivo* data using the $f_{ub\ in\ vivo}$ (0.7) and the $f_{ub\ in\ vitro}$ (0.29), quantified as described in the materials and methods section, to correct for differences in protein binding in the *in vitro* and *in vivo* situation. The ED_{50} values for PQ derived from the *in vivo* dose response curves obtained range from 9.3 to 17.8 mg/kg bw for the data based on the RLE-6TN cytotoxicity studies, while the ED_{50} was predicted at 35.3 mg/kg bw based on the L2 cytotoxicity data (Fig. 8a). For human, all five *in vitro* data sets obtained in A594 cells were translated to *in vivo* data using the $f_{ub\ in\ vivo}$ (0.65) and the $f_{ub\ in\ vitro}$ (0.27) to correct for differences in protein binding in the *in vitro* and *in vivo* situation (Fig. 8b). There are clear differences in the *in vitro* EC_{50} values and as a result also in the predicted ED_{50} values when based on 24 or 48 h exposure duration. Using 24 h exposure *in vitro* data the predicted ED_{50} values for PQ range from 32.5 to 72.2 mg/kg bw while based on the *in vitro* data obtained upon 48 h exposure the ED_{50} values are 4 – 12 fold lower ranging from 5.9 to 7.9 mg/kg bw.

3.6. Predicted point of departure for safety assessment

Based on the predicted acute *in vivo* toxicity data sets $BMDL_{50}$ $BMDU_{50}$ values were generated to allow a comparison to available *in vivo* toxicity data. There were data available on LD_{50} values especially in rat while some studies reported a human value (Bailey and White, 1965; Clark et al. 1966; Duerden, 1994; Kimbrough and Gaines, 1970; Mehani, 1972; Murray and Gibson, 1974; Sharp et al. 1972; Shirasu, 1977). As shown in Fig. 9 the predicted $BMDL_{50}$ to $BMDU_{50}$ ranges based on the rat *in vitro* cytotoxicity data are conservative compared to the reported *in vivo* LD_{50} data with the prediction by Chen et al. (2012) using the L2 cell line being 4.1-fold lower and closest to the average *in vivo* LD_{50} values, the latter varying up to 8-fold between the different *in vivo* studies.

The human A594 cytotoxicity assays in combination with the human PBK model resulted in predictions for the $BMDL_{50}$ $BMDU_{50}$ range in human that were in line with the limited reported LD_{50} values for human (Fig. 10). The predictions overall vary between 3.2 and 84.9 mg/kg bw while the available human *in vivo* data vary between 3 and 60 mg/kg bw pointing at the suitability of the A594 cell line to predict PQ toxicity.

4. Discussion

The present study aimed at evaluating a new approach methodology (NAM) for predicting the acute toxicity of PQ. The NAM consisted of using PBK models that included *in vitro* kinetic data for active renal excretion *via* the OCT2 transporter and *in vitro* cytotoxicity curves obtained in rat and human alveolar cell lines that were translated to *in vivo* dose response curves by applying PBK model based reverse dosimetry. From the predicted *in vivo* dose-response curves $BMDL_{50}$ to $BMDU_{50}$ ranges were derived and compared to the *in vivo* reported LD_{50} values in rat and human.

A secondary aim of the study was to provide a further proof of principle for using the *in vitro* cell line SA7K to obtain PBK parameters for transporter kinetics for OCT2 mediated renal excretion using PQ as the model compound. Although in the SA7K cells there was net cellular uptake *via* OCT2, an apparent equilibrium was reached already within a

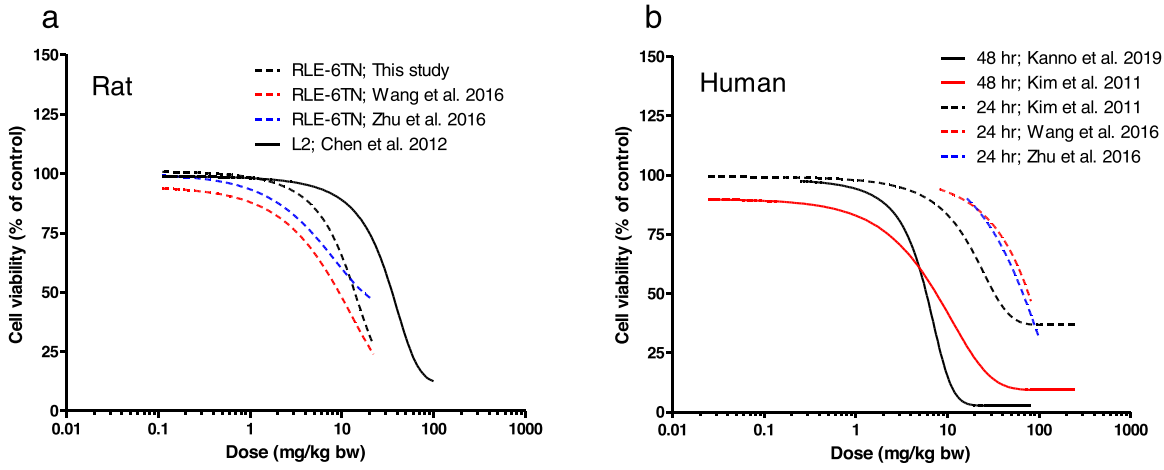

Fig. 8. Predicted dose-response curves for PQ obtained using (a) data from rat *in vitro* RLE-6TN and L2 cytotoxicity assays and the rat oral PBK model and (b) data from human *in vitro* A594 cytotoxicity assays and the human PBK model. The *in vitro* data used to make the predictions were (a) derived from either the present study (black striped line; ED_{50}: 13.3 mg/kg bw) or from literature as reported by Wang et al. (2016) (red striped line; ED_{50}: 9.3 mg/kg bw) and Zhu et al. (2016) (blue striped line; ED_{50}: 17.8 mg/kg bw) and data from an *in vitro* L2 cytotoxicity assay reported by Chen et al. (2012) (black solid line; ED_{50}: 35.3 mg/kg bw) and (b) previously reported by Kanno et al. (2019) (black solid line; ED_{50}: 5.9 mg/kg bw), Kim et al. (2011) (48 hr: red solid line; ED_{50}: 7.9 mg/kg bw and 24 hr: black striped line; ED_{50}: 32.5 mg/kg bw) and Wang et al. (2016) (red striped line; ED_{50}: 74.7 mg/kg bw) Zhu et al. (2016) (blue striped line; ED_{50}: 67.4 mg/kg bw). Data points represent the mean ± SD; n = 3–6.

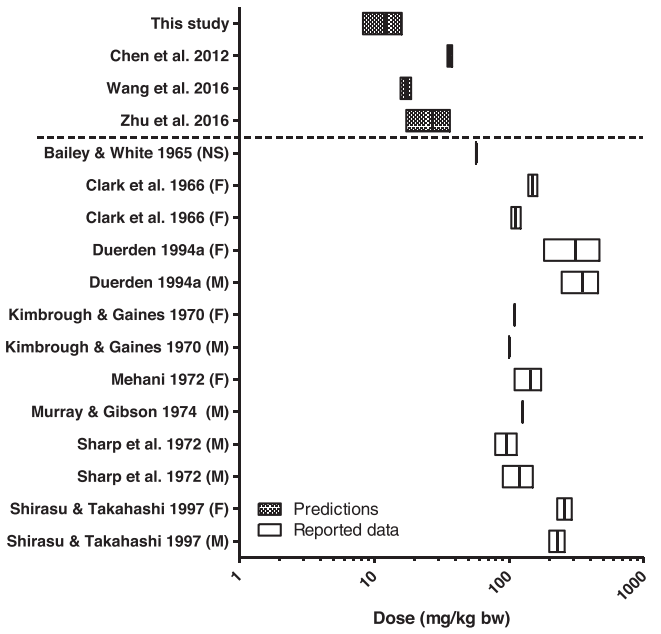

Fig. 9. Comparison of predicted $BMDL_{50}$ to $BMDU_{50}$ values for PQ in rat obtained by PBK model based QIVIVE of *in vitro* cytotoxicity data obtained in RLE-6TN and L2 cells (data obtained in this study and reported by Wang et al. (2016), Zhu et al. (2016) and Chen et al. (2012)) depicted by the chequered bars and literature reported *in vivo* rat LD_{50} values (open bars). F; female, M; male, NS; not specified.

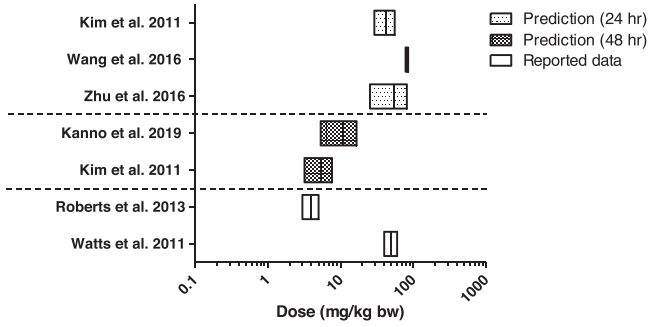

Fig. 10. Comparison of predicted $BMDL_{50}$ to $BMDU_{50}$ values for PQ in human obtained by PBK model based QIVIVE of *in vitro* cytotoxicity data obtained in A594 cells (data reported by Kanno et al. (2019), Kim et al. (2011), Wang et al. (2016) and Zhu et al. (2016)) depicted by the dotted bars (exposure 24 h) and the chequered bars (exposure 48 hr) and the literature reported *in vivo* human LD_{50} values for acute exposure (open bars).

minute, hampering use of the cell line to generate a linear uptake of PQ in time. As a result, Vmax or Km could not be determined from concentration-dependent uptake studies. Whether this fast equilibrium is due to efficient cellular excretion balancing the OCT2 mediated uptake, possibly *via* MATE, remains open for further investigation (Chen et al. 2007). Thus the OCT2 mediated transport was included in the PBK model based on kinetic data reported in literature and obtained in a HEK293 OCT2 transfected model.

The contribution of OCT2 transport to the total renal clearance of PQ as predicted by the PQ kinetic data appeared to amount to 73% of the total renal excretion achieved *via* glomerular filtration and active OCT2 mediated excretion at low dose levels where OCT2 transport was not saturated. The OCT2 contribution to PQ excretion was predicted to decrease upon higher dose levels when saturation occurs. The derived percentage was only slightly lower than what was observed for the contribution of OCT2 transport in our previous reported work on MQ, where active OCT2 mediated excretion amounted to 85% of the total excretion (Noorlander et al. 2021b).

The Vmax of OCT2 mediated PQ transport in HEK293 cells overexpressing OCT2 was scaled from the *in vitro* to the *in vivo* situation in a way similar to what was done previously for the OCT2 mediated Vmax for transport of MQ in SA7K cells (Noorlander et al. 2021b). A three step scaling factor was derived including 1) the amount of protein per gram kidney, 2) a correction for the location of the OCT2 transporter in the kidney in only the kidney cortex (70% of whole kidney) and 3) the differences between the *in vitro* cell system and the *in vivo* situation including: i) the difference in expression of the OCT2 transporter in the HEK293 cells overexpressing human OCT2 as compared to the *in vivo* expression in rat renal cells (Hayer-Zillgen et al. 2002; Koepsell et al. 2003), ii) the species differences in transporters involved in the *in vitro* model and the *in vivo* situation being OCT2 in human and OCT1, OCT2 and OCT3 in rat kidney (Chu et al. 2013; Slitt et al. 2002), iii) the difference in the negative membrane potential between *in vitro* and *in vivo* known to affect transporter efficiency (Kumar et al. 2018). The factor of 5.5 defined as extra scaling factor by comparison of predictions based on the transfected human HEK293 cell line and rat *in vivo data* accounts for all these three factors.

Another way to scale from HEK293 cells with overexpression of a transporter of interest to the *in vivo* situation is to look at previously reported work where the relative expression factor (REF) and the relative activity factor (RAF) were defined to use *in vitro* transporter kinetic data to model *in vivo* biliary excretion (Chan et al. 2019; Izumi et al. 2018; Jamei et al. 2014; Kunze et al. 2014; Poirier et al. 2009). More recently, these REF and RAF values have been successfully applied in renal excretion *via* OAT (Kumar et al. 2020; Mathialagan et al. 2017). Defining a REF is based on quantifying the OCT2 transporter protein levels in the HEK293 cells (or SA7K cells) and in rat/human kidney cells with proteomics. The difference can be used to define a scaling factor. In addition, considering that it would be even more accurate to base the comparison on activity rather than on protein expression levels, the RAF is defined by using a probe substrate for the transporter of interest in both the *in vitro* and *in vivo* situation. However, up until now for OCT2 no probe substrate has been defined (Burt et al. 2016). As a result reported RAF values for OCT2 transport result from fitting predictions to experimental data, just as done for the scaling factor in the present study.

Based on the sensitivity analysis performed (Fig.A2 Supplementary materials) the model outcome was most influenced by the fraction absorbed and the fraction unbound in blood. Thus, to further refine the model predictions and reduce variability and uncertainty especially these parameters should be quantified with high accuracy. The latter is especially important when studying the effects of longer term instead of acute exposure since Campbell et al. (2021) reported that the fraction unbound of PQ in both blood and plasma changes over time (measured for 14 days).

The PBK model predictions for the lethal dose ($BMDL_{50}$-$BMDU_{50}$ range) for rats were conservative compared to the *in vivo* reported data. It also revealed humans to be more sensitive to PQ than rat, which was in accordance with the reported LD_{50} values (Lin et al. 2021). Especially for human the predicted $BMDL_{50}$-$BMDU_{50}$ for acute toxicity of PQ matched the available LD_{50} values. For rat the predictions were on the conservative side, which may in part be due to the relevance of the *in vitro* cell model for the *in vivo* endpoint.

Information on the sensitivity of rat *versus* human lung cell lines to PQ can be derived from the EC_{50} values presented in Figs. 3 and 4 comparing the values obtained upon 24 h exposure for the rat RLE-6TN and human A549 cells for which several values are available. The average of these EC_{50} values reveals that the human A549 cells appears on average 5.5-fold less sensitive than the rat RLE-6TN cells. Given this *in vitro* difference it is also of interest to note that the difference in the predicted ED_{50} values for PQ between rat and human, amount to on average 6.1-fold when based on the predictions from the rat RLE-6TN and human A549 cell lines. Comparison of these fold differences in

the *in vitro* and predicted *in vivo* situation indicates that the 6.1 fold lower predicted ED_{50} for rat than human, can mainly be ascribed to a 5.5 fold species dependent difference in the toxicodynamics and is less substantially influenced by interspecies differences in toxicokinetics.

The *in vivo* toxicity of PQ is described by an adverse outcome pathway where the molecular initiating event starts in the lungs, therefore an alveolar *in vitro* model (RLE-6TN and L2) was used to measure cytotoxicity. Although the acute toxicity of PQ starts in the lung where in the first few hours it manifests as acute pulmonary oedema and early lung damage through redox cycling the main cause of death, however, respiratory failure by pulmonary fibrosis and can occur up until 7–14 days after PQ ingestion (Roberts JRRR, 2013). Therefore, a lung fibrotic *in vitro* model could have been a better alternative in mimicking the *in vivo* endpoint. Fibrotic *in vitro* models come with high complexity due to the interplay between many factors that cause fibrosis (Kiener et al. 2021; Martinez et al. 2017; Wolters et al. 2014). It is therefore that 3D models such as precision cut lung slices and lung on a chip are preferred over 2D models, which are too static forcing fibroblasts to polarize (Sundarakrishnan et al. 2018). 2D models are also incapable of replicating the complex gradient of soluble signalling molecules observed *in vivo* and can also not mimic the different cell-cell and cell-matrix interactions experienced by cells within the normal lung (Kiener et al. 2021; Vazquez-Armendariz et al. 2022). It might be interesting for future research to investigate whether a 3D lung fibrotic model for rat would result in predictions less sensitive compared to the predictions based on cytotoxicity corroborating the reported LD_{50} data.

In this study, the developed PBK model for PQ was capable of predicting the time-dependent blood concentration of PQ upon oral administration at a non-toxic dose. Previously published PBK models on PQ had similar success but were more extensively parameterized (Campbell et al. 2021; Stevens et al. 2021) or were even less parameterized (Lohitnavy et al. 2017) and in all cases did not take active renal excretion into account fitting a model with only glomerular filtration to the reported *in vivo* data. The present model was also able to make adequate predictions for the *in vivo* acute toxicity of PQ especially in humans. Thus, proof of principle was provided for the developed NAM showing how to include *in vitro* obtained active excretion in PBK modelling and how to apply the model for QIVIVE to predict the acute *in vivo* toxicity in both rat and human, using PQ as the model compound.

Funding

This work was supported by BASF SE (grant number: 6139030400).

Declaration of Competing Interest

The authors declare that they have no known competing financial interests or personal relationships that could have appeared to influence the work reported in this paper.

Data Availability

Data will be made available on request.

Acknowledgements

The authors acknowledge the contributions made in an initial stage of the work by MSc student Liza Weijers.

Appendix A. Supporting information

Supplementary data associated with this article can be found in the online version at doi:10.1016/j.toxlet.2023.10.001.

References

Bailey, G.W., White, J.L., 1965. Herbicides: a compilation of their physical, chemical, and biological properties. Residue Rev. 10, 97–122. https://doi.org/10.1007/978-1-4615-8398-1_5.

Brown, R.P., Delp, M.D., Lindstedt, S.L., Rhomberg, L.R., Beliles, R.P., 1997. Physiological parameter values for physiologically based pharmacokinetic models. Toxicol. Ind. Health 13 (4), 407–484. https://doi.org/10.1177/074823379701300401.

Burt, H.J., Neuhoff, S., Almond, L., et al., 2016. Metformin and cimetidine: Physiologically based pharmacokinetic modelling to investigate transporter mediated drug-drug interactions. Eur. J. Pharm. Sci. 88, 70–82. https://doi.org/10.1016/j.ejps.2016.03.020.

Campbell J.L., Jr., Travis K.Z., Clewell H.J., 3rd, et al. (2021) Integration of paraquat pharmacokinetic data across species using PBPK modelling. Toxicol Appl Pharmacol 417:115462 doi:10.1016/j.taap.2021.115462.

Chan, B.S., Lazzaro, V.A., Seale, J.P., Duggin, G.G., 1998. The renal excretory mechanisms and the role of organic cations in modulating the renal handling of paraquat. Pharm. Ther. 79 (3), 193–203. https://doi.org/10.1016/s0163-7258(98)00015-1.

Chan, B.S., Seale, J.P., Duggin, G.G., 1997. The mechanism of excretion of paraquat in rats. Toxicol. Lett. 90 (1), 1–9. https://doi.org/10.1016/s0378-4274(96)03820-9.

Chan, J.C.Y., Tan, S.P.F., Upton, Z., Chan, E.C.Y., 2019. Bottom-up physiologically-based biokinetic modelling as an alternative to animal testing. ALTEX 36 (4), 597–612. https://doi.org/10.14573/altex.1812051.

Chen, Y., Teranishi, K., Li, S., et al., 2009. Genetic variants in multidrug and toxic compound extrusion-1, hMATE1, alter transport function. Pharm. J. 9 (2), 127–136. https://doi.org/10.1038/tpj.2008.19.

Chen, Y., Zhang, S., Sorani, M., Giacomini, K.M., 2007. Transport of paraquat by human organic cation transporters and multidrug and toxic compound extrusion family. J. Pharm. Exp. Ther. 322 (2), 695–700. https://doi.org/10.1124/jpet.107.123554.

Chen, Y.W., Yang, Y.T., Hung, D.Z., Su, C.C., Chen, K.L., 2012. Paraquat induces lung alveolar epithelial cell apoptosis via Nrf-2-regulated mitochondrial dysfunction and ER stress. Arch. Toxicol. 86 (10), 1547–1558. https://doi.org/10.1007/s00204-012-0873-8.

Chu, X., Bleasby, K., Evers, R., 2013. Species differences in drug transporters and implications for translating preclinical findings to humans. Expert Opin. Drug Metab. Toxicol. 9 (3), 237–252. https://doi.org/10.1517/17425255.2013.741589.

Chui, Y.C., Poon, G., Law, F., 1988. Toxicokinetics and bioavailability of paraquat in rats following different routes of administration. Toxicol. Ind. Health 4 (2), 203–219. https://doi.org/10.1177/074823378800400205.

Clark, D.G., McElligott, T.F., Hurst, E.W., 1966. The toxicity of paraquat. Br. J. Ind. Med 23 (2), 126–132. https://doi.org/10.1136/oem.23.2.126.

Dean L. (2005) Chapter 1, Blood an the cells it contains. In: Blood groups and red cell antigens. National Center for Biotechnology Information (US). https://www.ncbi.nlm.nih.gov/books/NBK2263/ Accessed 23rd of May 2022.

Dinis-Oliveira, R.J., Duarte, J.A., Sanchez-Navarro, A., Remiao, F., Bastos, M.L., Carvalho, F., 2008. Paraquat poisonings: mechanisms of lung toxicity, clinical features, and treatment. Crit. Rev. Toxicol. 38 (1), 13–71. https://doi.org/10.1080/10408440701669959.

Duerden, L., 1994. Paraquat Dichloride Technical Concentrate: Acute Oral Toxicity to the Rat. Zeneca Central Toxicology Laboratory, U.K.

EPA U (2019) Paraquat Dichloride: Draft Human Health Risk Assessment in Support of Registration Review. p 103.

Evans, M.V., Andersen, M.E., 2000. Sensitivity analysis of a physiological model for 2,3,7,8-tetrachlorodibenzo-p-dioxin (TCDD): assessing the impact of specific model parameters on sequestration in liver and fat in the rat. Toxicol. Sci. 54 (1), 71–80. https://doi.org/10.1093/toxsci/54.1.71.

George, B., You, D., Joy, M.S., Aleksunes, L.M., 2017. Xenobiotic transporters and kidney injury. Adv. Drug Deliv. Rev. 116, 73–91. https://doi.org/10.1016/j.addr.2017.01.005.

Gulden, M., Morchel, S., Tahan, S., Seibert, H., 2002. Impact of protein binding on the availability and cytotoxic potency of organochlorine pesticides and chlorophenols in vitro. Toxicology 175 (1–3), 201–213. https://doi.org/10.1016/s0300-483x(02)00085-9.

Hacker, K., Maas, R., Kornhuber, J., Fromm, M.F., Zolk, O., 2015. Substrate-dependent inhibition of the human organic cation transporter OCT2: a comparison of metformin with experimental substrates. PLoS One 10 (9), e0136451. https://doi.org/10.1371/journal.pone.0136451.

Hayer-Zillgen, M., Bruss, M., Bonisch, H., 2002. Expression and pharmacological profile of the human organic cation transporters hOCT1, hOCT2 and hOCT3. Br. J. Pharm. 136 (6), 829–836. https://doi.org/10.1038/sj.bjp.0704785.

Houze, P., Baud, F.J., Mouy, R., Bismuth, C., Bourdon, R., Scherrmann, J.M., 1990. Toxicokinetics of paraquat in humans. Hum. Exp. Toxicol. 9 (1), 5–12. https://doi.org/10.1177/096032719000900103.

Izumi, S., Nozaki, Y., Kusuhara, H., et al., 2018. Relative activity factor (RAF)-based scaling of uptake clearance mediated by organic anion transporting polypeptide (OATP) 1B1 and OATP1B3 in human hepatocytes. Mol. Pharm. 15 (6), 2277–2288. https://doi.org/10.1021/acs.molpharmaceut.8b00138.

Jamei, M., Bajot, F., Neuhoff, S., et al., 2014. A mechanistic framework for in vitro-in vivo extrapolation of liver membrane transporters: prediction of drug-drug interaction between rosuvastatin and cyclosporine. Clin. Pharm. 53 (1), 73–87. https://doi.org/10.1007/s40262-013-0097-y.

Kanno, S., Hirano, S., Mukai, T., et al., 2019. Cellular uptake of paraquat determines subsequent toxicity including mitochondrial damage in lung epithelial cells. Leg. Med. 37, 7–14. https://doi.org/10.1016/j.legalmed.2018.11.008.

Kasteel, E.E.J., Lautz, L.S., Culot, M., Kramer, N.I., Zwartsen, A., 2021. Application of in vitro data in physiologically-based kinetic models for quantitative in vitro-in vivo extrapolation: A case-study for baclofen. Toxicol. Vitr. 76, 105223 https://doi.org/10.1016/j.tiv.2021.105223.

Kiener, M., Roldan, N., Machahua, C., et al., 2021. Human-based advanced in vitro approaches to investigate lung fibrosis and pulmonary effects of COVID-19. Front Med. 8, 644678 https://doi.org/10.3389/fmed.2021.644678.

Kim, H., Lee, S.W., Baek, K.M., Park, J.S., Min, J.H., 2011. Continuous hypoxia attenuates paraquat-induced cytotoxicity in the human A549 lung carcinoma cell line. Exp. Mol. Med. 43 (9), 494–500. https://doi.org/10.3858/emm.2011.43.9.056.

Kimbrough, R.D., Gaines, T.B., 1970. Toxicity of paraquat to rats and its effect on rat lungs. Toxicol. Appl. Pharm. 17 (3), 679–690. https://doi.org/10.1016/0041-008x(70)90042-6.

Koepsell, H., Schmitt, B.M., Gorboulev, V., 2003. Organic cation transporters. Rev. Physiol. Biochem Pharm. 150, 36–90. https://doi.org/10.1007/s10254-003-0017-x.

Kumar, A.R., Prasad, B., Bhatt, D.K., Mathialagan, S., Varma, M.V.S., Unadkat, J.D., 2020. In vivo-to-in vitro extrapolation of transporter-mediated renal clearance: relative expression factor versus relative activity factor approach. Drug Metab. Dispos. 49 (6), 470–478. https://doi.org/10.1124/dmd.121.000367.

Kumar, V., Yin, J., Billington, S., et al., 2018. The importance of incorporating OCT2 plasma membrane expression and membrane potential in IVIVE of metformin renal secretory clearance. Drug Metab. Dispos. 46 (10), 1441–1445. https://doi.org/10.1124/dmd.118.082313.

Kunze, A., Huwyler, J., Camenisch, G., Poller, B., 2014. Prediction of organic anion-transporting polypeptide 1B1- and 1B3-mediated hepatic uptake of statins based on transporter protein expression and activity data. Drug Metab. Dispos. 42 (9), 1514–1521. https://doi.org/10.1124/dmd.114.058412.

Li, S., Zhao, J., Huang, R., et al., 2017. Development and application of human renal proximal tubule epithelial cells for assessment of compound toxicity. Curr. Chem. Genom. Transl. Med. 11, 19–30. https://doi.org/10.2174/2213988501711010019.

Lin, C.C., Hsu, K.H., Shih, C.P., Chang, G.J., 2021. Hemodynamic and electromechanical effects of paraquat in rat heart. PLoS One 16 (4), e0234591. https://doi.org/10.1371/journal.pone.0234591.

Lock, E.A.W., M. F, 2010. Paraquat. In: Krieger, R. (Ed.), Hayes' Handbook of Pesticide Toxicology. Elsevier Inc.

Lohitnavy, M., Chitsakhon, A., Jomprasert, K., Lohitnavy, O., Reisfeld, B., 2017. Development of a physiologically based pharmacokinetic model of paraquat. Annu Int Conf. IEEE Eng. Med Biol. Soc. 2017, 2732–2735. https://doi.org/10.1109/EMBC.2017.8037422.

Martinez, F.J., Collard, H.R., Pardo, A., et al., 2017. Idiopathic pulmonary fibrosis. Nat. Rev. Dis. Prim. 3, 17074. https://doi.org/10.1038/nrdp.2017.74.

Martinez, M.N., 2011. Factors influencing the use and interpretation of animal models in the development of parenteral drug delivery systems. AAPS J. 13 (4), 632–649. https://doi.org/10.1208/s12248-011-9303-8.

Mathew J., Sankar P., Varacallo M. (2022) Physiology, Blood Plasma StatPearls. Treasure Island (FL).

Mathialagan, S., Piotrowski, M.A., Tess, D.A., Feng, B., Litchfield, J., Varma, M.V., 2017. Quantitative prediction of human renal clearance and drug-drug interactions of organic anion transporter substrates using in vitro transport data: a relative activity factor approach. Drug Metab. Dispos. 45 (4), 409–417. https://doi.org/10.1124/dmd.116.074294.

Mehani, S., 1972. The toxic effect of paraquat in rabbits and rats. Ain Shams Med. J. 23, 3.

Muhamad, H., Ismail, B.S., Sameni, M., Mat, N., 2011. Adsorption study of 14C-paraquat in two Malaysian agricultural soils. Environ. Monit. Assess. 176 (1–4), 43–50. https://doi.org/10.1007/s10661-010-1565-6.

Murray, R.E., Gibson, J.E., 1974. Paraquat disposition in rats, guinea pigs and monkeys. Toxicol. Appl. Pharm. 27 (2), 283–291. https://doi.org/10.1016/0041-008x(74)90199-9.

Noorlander, A., Fabian, E., van Ravenzwaay, B., Rietjens, I., 2021a. Novel testing strategy for prediction of rat biliary excretion of intravenously administered estradiol-17beta glucuronide. Arch. Toxicol. 95 (1), 91–102. https://doi.org/10.1007/s00204-020-02908-x.

Noorlander, A., Wesseling, S., Rietjens, I., van Ravenzwaay, B., 2021b. Incorporating renal excretion via the OCT2 transporter in physiologically based kinetic modelling to predict in vivo kinetics of mepiquat in rat. Toxicol. Lett. 343, 34–43. https://doi.org/10.1016/j.toxlet.2021.02.013.

Noorlander, A., Zhang, M., van Ravenzwaay, B., Rietjens, I., 2022. Use of physiologically based kinetic modeling-facilitated reverse dosimetry to predict in vivo acute toxicity of tetrodotoxin in rodents. Toxicol. Sci. 187 (1), 127–138. https://doi.org/10.1093/toxsci/kfac022.

Pizzutti, I.R., Vela, G.M., de Kok, A., et al., 2016. Determination of paraquat and diquat: LC-MS method optimization and validation. Food Chem. 209, 248–255. https://doi.org/10.1016/j.foodchem.2016.04.069.

Poirier, A., Cascais, A.C., Funk, C., Lave, T., 2009. Prediction of pharmacokinetic profile of valsartan in human based on in vitro uptake transport data. J. Pharm. Pharm. 36 (6), 585–611. https://doi.org/10.1007/s10928-009-9139-3.

Proudfoot, A.T., Stewart, M.S., Levitt, T., Widdop, B., 1979. Paraquat poisoning: significance of plasma-paraquat concentrations. Lancet 2 (8138), 330–332. https://doi.org/10.1016/s0140-6736(79)90345-3.

Punt, A., Pinckaers, N., Peijnenburg, A., Louisse, J., 2020. Development of a web-based toolbox to support quantitative in-vitro-to-in-vivo extrapolations (QIVIVE) within nonanimal testing strategies. Chem. Res Toxicol. https://doi.org/10.1021/acs.chemrestox.0c00307.

Rietjens I., Ning J., Chen L., Wesseling S., Strikwold M., Louisse J. (2019) Selecting the dose metric in reverse dosimetry based QIVIVE: Reply to 'Comment on 'Use of an in vitro-in silico testing strategy to predict inter-species and inter-ethnic human differences in liver toxicity of the pyrrolizidine alkaloids lasiocarpine and riddelliine' by Ning et al., Arch Toxicol doi: https://doi.org/10.1007/s00204–019-02397–7', Arch Toxicol doi: https://doi.org/10.1007/s0020 4–019-02421-w. Arch Toxicol 93 (5):1467–1469 doi:10.1007/s00204–019-02438–1.

Roberts JRRR, J., 2013. Recognition and Management of Pesticide Poisonings, 6th ed.,. Environmental protection agency, United states of America.

Rodgers, T., Rowland, M., 2006. Physiologically based pharmacokinetic modelling 2: predicting the tissue distribution of acids, very weak bases, neutrals and zwitterions. J. Pharm. Sci. 95 (6), 1238–1257. https://doi.org/10.1002/jps.20502.

Samai, M., Hague, T., Naughton, D.P., Gard, P.R., Chatterjee, P.K., 2008. Reduction of paraquat-induced renal cytotoxicity by manganese and copper complexes of EGTA and EHPG. Free Radic. Biol. Med. 44 (4), 711–721. https://doi.org/10.1016/j.freeradbiomed.2007.11.001.

Sawada, Y., Yamamoto, I., Hirokane, T., Nagai, Y., Satoh, Y., Ueyama, M., 1988. Severity index of paraquat poisoning. Lancet 1 (8598), 1333. https://doi.org/10.1016/s0140-6736(88)92143-5.

Scherrmann, J.M., Houze, P., Bismuth, C., Bourdon, R., 1987. Prognostic value of plasma and urine paraquat concentration. Hum. Toxicol. 6 (1), 91–93. https://doi.org/10.1177/096032718700600116.

Sharp, C.W., Ottolenghi, A., Posner, H.S., 1972. Correlation of paraquat toxicity with tissue concentrations and weight loss of the rat. Toxicol. Appl. Pharm. 22 (2), 241–251. https://doi.org/10.1016/0041-008x(72)90174-3.

Shirasu Y.T., K (1977) Study report: acute toxicity of AT-5 in rat and mouse. Institute of Environmental Toxicology, Unpublished.

Slitt, A.L., Cherrington, N.J., Hartley, D.P., Leazer, T.M., Klaassen, C.D., 2002. Tissue distribution and renal developmental changes in rat organic cation transporter mRNA levels. Drug Metab. Dispos. 30 (2), 212–219. https://doi.org/10.1124/dmd.30.2.212.

Stevens, A.J., Campbell Jr., J.L., Travis, K.Z., et al., 2021. Paraquat pharmacokinetics in primates and extrapolation to humans. Toxicol. Appl. Pharm. 417, 115463 https://doi.org/10.1016/j.taap.2021.115463.

Strikwold, M., Spenkelink, B., de Haan, L.H.J., Woutersen, R.A., Punt, A., Rietjens, I., 2017. Integrating in vitro data and physiologically based kinetic (PBK) modelling to assess the in vivo potential developmental toxicity of a series of phenols. Arch. Toxicol. 91 (5), 2119–2133. https://doi.org/10.1007/s00204-016-1881-x.

Sundarakrishnan, A., Chen, Y., Black, L.D., Aldridge, B.B., Kaplan, D.L., 2018. Engineered cell and tissue models of pulmonary fibrosis. Adv. Drug Deliv. Rev. 129, 78–94. https://doi.org/10.1016/j.addr.2017.12.013.

van Tongeren, T.C.A., Moxon, T.E., Dent, M.P., Li, H., Carmichael, P.L., Rietjens, I., 2021. Next generation risk assessment of human exposure to anti-androgens using newly defined comparator compound values. Toxicol. Vitr. 73, 105132 https://doi.org/10.1016/j.tiv.2021.105132.

Vazquez-Armendariz, A.I., Barroso, M.M., El Agha, E., Herold, S., 2022. 3D in vitro models: novel insights into idiopathic pulmonary fibrosis pathophysiology and drug screening. Cells 11 (9). https://doi.org/10.3390/cells11091526.

Walton, K., Dorne, J.L., Renwick, A.G., 2004. Species-specific uncertainty factors for compounds eliminated principally by renal excretion in humans. Food Chem. Toxicol. 42 (2), 261–274. https://doi.org/10.1016/j.fct.2003.09.001.

Wang, J., Zhu, Y., Tan, J., Meng, X., Xie, H., Wang, R., 2016. Lysyl oxidase promotes epithelial-to-mesenchymal transition during paraquat-induced pulmonary fibrosis. Mol. Biosyst. 12 (2), 499–507. https://doi.org/10.1039/c5mb00698h.

Wang, Z., Gu, D., Sheng, L., Cai, J., 2018. Protective effect of anthocyanin on paraquat-induced apoptosis and epithelial-mesenchymal transition in alveolar type II cells. Med Sci. Monit. 24, 7980–7987. https://doi.org/10.12659/MSM.910730.

Watts M. (2011) Paraquat. Pesticide Action Network Asia and the Pacific, p 44.

Wolters, P.J., Collard, H.R., Jones, K.D., 2014. Pathogenesis of idiopathic pulmonary fibrosis. Annu Rev. Pathol. 9, 157–179. https://doi.org/10.1146/annurev-pathol-012513-104706.

Worley, R.R., Fisher, J., 2015. Application of physiologically-based pharmacokinetic modeling to explore the role of kidney transporters in renal reabsorption of perfluorooctanoic acid in the rat. Toxicol. Appl. Pharm. 289 (3), 428–441. https://doi.org/10.1016/j.taap.2015.10.017.

Zhu, Y., Tan, J., Xie, H., Wang, J., Meng, X., Wang, R., 2016. HIF-1alpha regulates EMT via the Snail and beta-catenin pathways in paraquat poisoning-induced early pulmonary fibrosis. J. Cell Mol. Med 20 (4), 688–697. https://doi.org/10.1111/jcmm.12769.